Progress In Electromagnetics Research, Vol. 124, 487–510, 2012

DOSIMETRY AND TEMPERATURE EVALUATIONS OF A 1800 MHz TEM CELL FOR IN VITRO EXPOSURE WITH STANDING WAVES

J. X. Zhao*, H. M. Lu, and J. Deng

School of Electronic Engineering, Xidian University, Xi'an 710071, China

Abstract—A 1800 MHz transverse electromagnetic wave (TEM) cell is introduced for experiments investigating effects on biological samples caused by the exposure from mobile communications. To characterize and quantify the exposure environment in the setup for standardized in vitro experiments, we evaluate the dosimetry and the exposure-induced temperature rise in cultured cells. The study is numerically based on the finite-difference time-domain (FDTD) formulation of the Maxwell equations and the finite-difference formulation of the bioheat transfer equation, with all algorithms and models strictly validated for accuracy. Two sample formations of cells are considered including the cell layer and the cell suspension cultured in the 35 mm Petri dish. The TEM cell is designed to establish standing waves with the maximum E field and the maximum H field, respectively, at the position of the Petri dish. The Petri dish is oriented to $\boldsymbol{E}$, $-\boldsymbol{E}$, $\boldsymbol{H}$, $\boldsymbol{k}$, and $-\boldsymbol{k}$ directions of the incident field, respectively, to receive the exposure. The specific absorption rate (SAR) is calculated in cells for 10 exposure arrangements combined from the maximum fields and Petri dish orientations. A comparison determines the best arrangement with the highest exposure efficiency and the lowest exposure heterogeneity. The dosimetry and the exposure-induced temperature rise in cells are evaluated for the selected arrangement. To avoid thermal reactions caused by overheating, the maximum temperature rises in cells are recorded during the exposure. Based on the records, the temperature control is performed by setting limits to the exposure duration. We introduce a method to further reduce the exposure heterogeneity and evaluate the influence of the Petri dish holder on the dosimetry and temperature rise. The study compares the TEM cell to the waveguide, as well as the standing wave exposure

Received 12 September 2011, Accepted 6 February 2012, Scheduled 12 February 2012

* Corresponding author: Jian Xun Zhao (jxzhao@xidian.edu.cn).

to the propagating wave exposure. The TEM cell and the selected arrangement of the standing wave exposure improve the exposure quality over the traditional methods, with increased efficiency and decreased heterogeneity of the exposure.

1. INTRODUCTION

The transverse electromagnetic wave (TEM) cell and the waveguide are two typical exposure setups used to study in vitro and in vivo effects of electromagnetic irradiation at mobile frequencies centered at 900 MHz and 1800 MHz [1]. Compared to the widely used waveguide, the TEM cell generates a uniform, planar wave in the sample space for experiments fulfilling the suggested exposure standards, so that the results are comparable to those from other experiments under the same exposure protocol [2, 3]. Successful dosimetry studies are available in the literature regarding to TEM cells loaded with biological samples at frequencies around 900 MHz [4].

At mobile frequencies, the exposure dosimetry is traditionally quantified as the specific absorption rate (SAR), which is defined as the absorbed electromagnetic power divided by the mass of the biological sample. For in vivo experiments on the whole body, the dosimetry usually uses the body-averaged SAR. In view of the inhomogeneous power absorption, 10-g SAR is used to quantify the power absorbed in every 10 g of the tissue. 10-g SAR is also the unit used by safety standards to describe the exposure on the head and brain, etc. [5, 6]. However, for in vitro experiments on cultured cells, the biological sample is far less than 10 g. Therefore, the SAR is quantified as its distribution in cells. Based on the mean and standard deviation (SD) of the SAR distribution, the exposure efficiency and heterogeneity are determined to describe the exposure quality [7].

In direct proportion to the mean SAR, the exposure efficiency is the ratio of the absorbed power in the cell culture to the input power of the setup. Higher efficiency means fewer burdens on the power source. To maximize the count of cells subjecting to the same exposure intensity, low exposure heterogeneity is desired in cells. For in vitro experiments, the heterogeneity is suggested to be no more than 30%, as measured by the SAR SD [8]. Due to the inherent SAR distribution in cells, it is difficult to change the exposure efficiency and heterogeneity by tunable devices. However, the SAR distribution changes greatly with different arrangements of the exposure, such as making use of various exposure setups, using the standing wave and the propagating wave, selecting different sample containers, adjusting the sample position, and changing the volume of the culture medium,

etc. [9]. This makes it possible to comparatively select the desired arrangement of the best exposure quality with the highest efficiency and the lowest heterogeneity. The temperature rise in the cell culture is more significant with increased exposure efficiency. In order to inhibit possible thermal effects for the observation of purely nonthermal effects, as well as to experimentally measure the SAR by temperature detection, a tight temperature control and evaluation are necessary supports to the experiment quality [10].

The influence of the exposure arrangement on the mean SAR and SAR SD has been thoroughly studied for the waveguide at 1800 MHz [11]. However, for the 1800 MHz TEM cell, a systematic solution to the dosimetric and thermal problems is still in request. Previous studies are limited to the exposure of propagating and standing waves at lower frequencies around 900 MHz [12–14].

In this paper, we study the dosimetry and temperature rise in cells cultured in the 35 mm Petri dish mounted in a designed 1800 MHz TEM cell. 10 exposure arrangements are analyzed systematically, including the standing wave exposures with the maximum E field and the maximum H field, as well as $\boldsymbol{E}$, $-\boldsymbol{E}$, $\boldsymbol{H}$, $\boldsymbol{k}$, and $-\boldsymbol{k}$ orientations of the Petri dish. The SAR in cells is calculated by using the finite-difference time-domain (FDTD) method for each exposure arrangement. The mean SARs and SAR SDs in the cell layer and cell suspension are derived from the SAR distribution and the best exposure arrangement is selected by comparing the exposure efficiency and heterogeneity. For the selected arrangement, we characterize the SAR in cells for dosimetric quantification of the exposure in the TEM cell. Using the finite-difference method of the bioheat transfer equation, we calculate the exposure-induced temperature rise and quantify the limits to the input power for the temperature control of the in vitro environment. Double-source exposure and selected cell sampling are proposed for the experimental application to improve the exposure quality. Recommendations about the holder of the Petri dish are provided to minimize its influence on the dosimetric and thermal environments. The TEM cell is compared to the waveguide on the dosimetric and thermal performances. Another comparison is made with respect to the exposure efficiency and heterogeneity between the standing wave exposure and the propagating wave exposure.

2. EXPOSURE SETUP

The geometry of the TEM cell is shown in Fig. 1(a). The thickness of the plates is 2.0 mm. The setup is designed to work at the frequency of 1800 MHz. The propagation distance from the source to the load is two

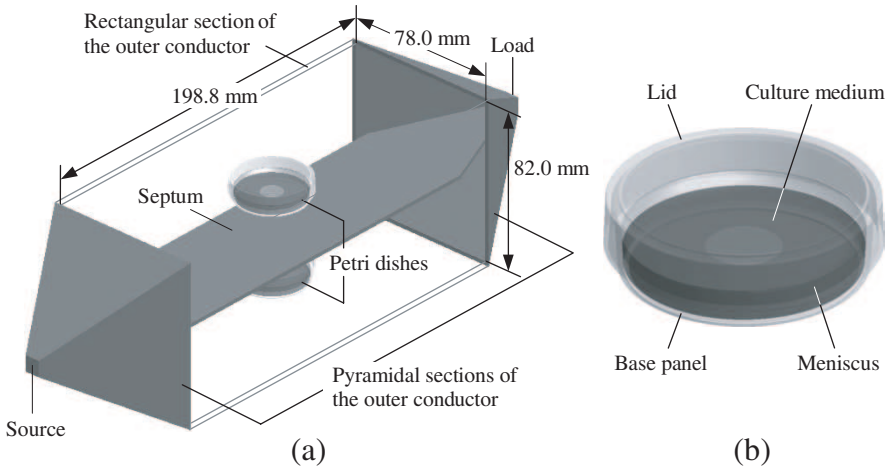

Figure 1. Exposure setup. (a) 1800 MHz TEM cell with two Petri dishes $\boldsymbol{E}$ and $-\boldsymbol{E}$ orientated, respectively. (b) Detailed geometry of the 35 mm Petri dish and culture medium.

wavelengths to build a standing wave with 4 loops. The transversal dimensions of the rectangular section are calculated to hold the Petri dish in the area of quasi-uniform exposure and to avoid the excitation of TE_{10} and other higher-order modes [15].

The source and load are added to both ends of the TEM cell. The source is a sinusoidal voltage at the frequency of 1800 MHz. The internal resistance is 50 Ω. The source generates the forward propagating wave. A standing wave is established with the backward propagating wave fully reflected from the load. There are two types of load to perform the full-wave reflection, namely, an open end and a short end. The reflected waves are 180° out of phase between the two loads and the standing waves are shifted by a quarter of the wavelength in the field distribution along the axis of the TEM cell. Since the length of the TEM cell is designed for 4 loops, the open end produces a standing wave with the maximum E field at the center, whereas the short end produces a standing wave with the maximum H field at the center.

The limited space of the 1800 MHz setup allows for cell containers of small sizes, such as the 35 mm Petri dish or small culture plates. The 35 mm Petri dish (Corning 430165, USA) is used in the study, as shown in Fig. 1(b). The Petri dish is originally filled with 2.68 ml culture medium [Dulbecco's modified eagle's medium (DMEM)]. The size of the Petri dish and the volume of the culture medium are selected because they are used by a majority of experimental studies reported in

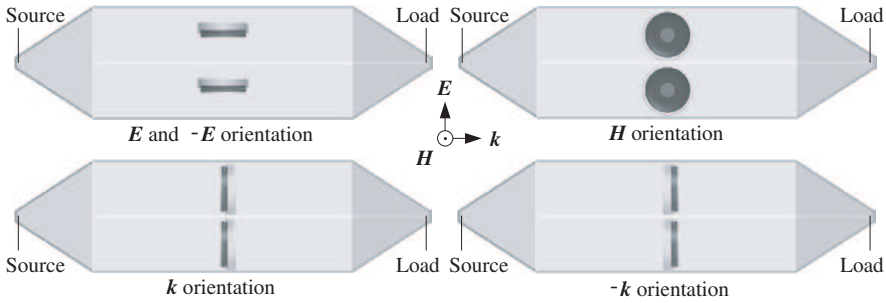

Figure 2. $\boldsymbol{E}$, $-\boldsymbol{E}$, $\boldsymbol{H}$, $\boldsymbol{k}$, and $-\boldsymbol{k}$ orientated Petri dishes at both centers of the upper and lower half-spaces of the TEM cell. Directions of $\boldsymbol{E}$, $\boldsymbol{H}$, and $\boldsymbol{k}$ vectors of the incident wave are shown.

the literature. We consider the meniscus geometry by using its profile equation since previous studies have proved the strong influence of the meniscus surface of the liquid on the dosimetry [16]. The dielectric and thermal properties of cells and the culture medium are very close and assumed as identical. Dosimetric and thermal results at the bottom of the culture medium represents those of the cell layer, whereas results of the cell suspension are collected from the entire medium.

As shown in Fig. 2, two Petri dishes are mounted into the TEM cell for simultaneous exposure. Each Petri dish is placed by positioning the center of the cell culture (that without the meniscus) at the center of the upper or lower half-space of the cavity, where the maximum field of the standing wave is established. Five directions of the Petri dish are selectable, namely, $\boldsymbol{E}$, $-\boldsymbol{E}$, $\boldsymbol{H}$, $\boldsymbol{k}$, and $-\boldsymbol{k}$ orientations. The orientation is defined by considering the largest surface of the cell culture with respect to the directions of the fields and the power flux of the incident wave. The maximum fields and Petri dish orientations combine into 10 exposure arrangements for dosimetry comparison.

3. NUMERICAL METHODS

The standing wave and the SAR distribution in cells are calculated by the FDTD method, with mesh models of the TEM cell and the Petri dish [17]. The exposure-induced temperature rise in the cell culture is calculated by using the bioheat transfer equation [18]. The temperature rise is assumed to happen after the transient establishment of the SAR distribution. Therefore, the FDTD calculation is performed first to provide the SAR data for the following bioheat calculation of the temperature rise.

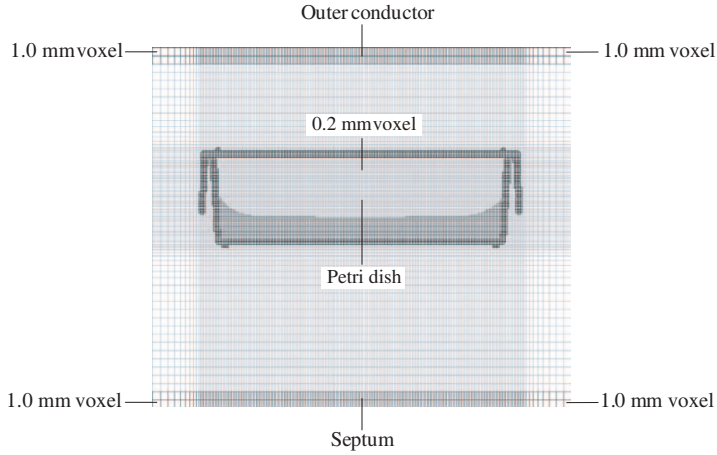

Figure 3. Cross section of the FDTD model where the voxel dimension varies between 0.2 mm and 1.0 mm from the inside to the outside of the Petri dish. This dish lies in the upper half-space of the TEM cell and orientated in the E direction.

3.1. FDTD Calculation

The FDTD mesh model of the TEM cell is made by 1.0 mm voxels. The staircase effect is neglected since the voxel size is only 1/167 of the wavelength in the air. 0.2 mm voxels are used to fit into the fine structure of the Petri dish. The voxel size shifts exponentially from 0.2 mm to 1.0 mm around the Petri dish, as shown in Fig. 3. The TEM cell is made of copper plates and has the property of the perfect electric conductor. Dielectric parameters of other materials are listed in Table 1. The permittivity and conductivity of the cell culture and those of the Petri dish are assigned to 12 edges of each corresponding voxel. The mass density of the cell culture is $1.0 \times 10^3\,\mathrm{kg/m^3}$. That of the Petri dish is $1.1 \times 10^3\,\mathrm{kg/m^3}$.

After the field distribution of the standing wave is completely stable, the SAR in cells is calculated by using the magnitude of the E field, $E_{\max}$, the material conductivity σ, and mass density ρ:

$$\mathrm{SAR} = \frac{\sigma}{2\rho} E_{\max}^2. \tag{1}$$

The calculation gives the SAR averaged in each voxel. The mean SAR and SAR SD of the cell layer and those of the cell suspension are statistically derived from voxels at the bottom and those of the entire cell culture.

The absorbed power is calculated by multiplying the mean SAR and the mass of cells. The input power of the TEM cell is calculated

Table 1. Dielectric and thermal parameters of materials at 1800 MHz and room temperature.

Material	Permittivity ε_r	Conductivity σ (S/m)	Specific heat C [J/(kg·°C)]
Cell culture	71	2.5	4200
Petri dish	2.5	0	1200

Material	Thermal conductivity K [W/(m·°C)]	Convection coefficient H [W/(m^2·°C)]
Cell culture	0.6	7.1
Petri dish	0.12	41

by using the same source and a 50 Ω matching load with the absence of Petri dishes. The difference between the input power and the absorbed power is the reflected power. The exposure efficiency is defined as the ratio of the absorbed power to the input power. The exposure heterogeneity is measured by the relative SD of the SAR distribution, i.e., the SAR SD divided by the mean SAR.

3.2. Bioheat Calculation

The bioheat transfer equation relates the local temperature rise to the heat conduction from the surroundings and the power absorption due to the exposure:

$$C\rho\frac{\partial T}{\partial t} = K\nabla^2 T + Q_v, \tag{2}$$

where C [J/(kg·°C)] is the specific heat, K [W/(m·°C)] is the thermal conductivity, $Q_v \approx \mathrm{SAR}\cdot\rho\,(\mathrm{W/m^3})$ is the power absorption density.

At the interface between the cell culture and the air, as well as the interface between the Petri dish and the air, the problem space is enclosed by using the convective boundary condition:

$$-K\frac{\partial T}{\partial t} = H(T_s - T_e), \tag{3}$$

where H [W/(m^2·°C)] is the convection coefficient determined by both media across the interface, T_s is the surface temperature of the cell culture or the Petri dish, and T_e represents the temperature of the surrounding air. Thermal parameters of materials are listed in Table 1 [19].

Equations (2) and (3) can be incorporated into one finite-differential formula for the numerical simulation [20]. The same voxel

model of the Petri dish and cell culture is used to calculate the temperature rise. The thermal parameters are assigned to each voxel where the voxel-averaged SAR is ready. The original temperature in the problem space is set to zero so that the result is the temperature rise.

4. ALGORITHM VALIDATION

The numerical study is supported by theoretical examinations of all algorithms and models involved in the complete exposure process. From the initial field generation to the final stabilized temperature rise in the biological sample, the validation is performed by three comparative tests on the calculation accuracy of the standing waves in the TEM cell, the SAR, and the temperature rise in cells.

4.1. Field Establishment

Prior to the placing of the Petri dish, the standing waves in the TEM cell are calculated and shown in Fig. 4. The peak fields in the pyramidal sections are not included to show up the field in the exposure area. Each pattern exhibits the 4-loop field distribution, as well as the maximum or minimum field generated at the position of the Petri dish. In the exposure area, the calculated field distributions of the E-field-maximum and H-field-maximum exposures are compared to the theoretical field distribution [21]. Close matches are found between the numerical results and the theoretical result in Fig. 5.

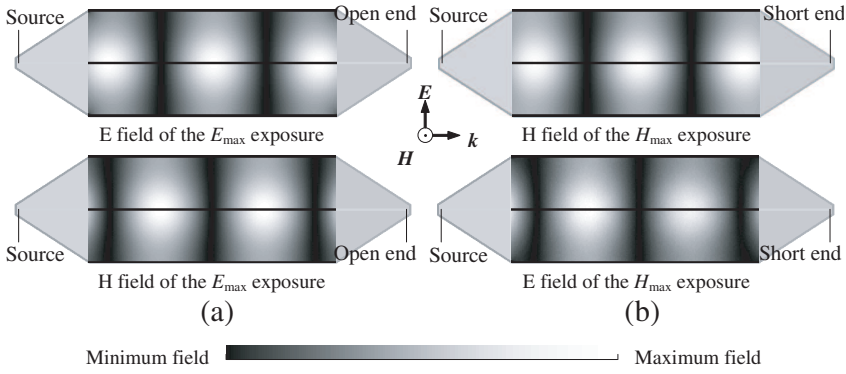

Figure 4. Field patterns across the axial section of the TEM cell. (a) E and H field distributions of the E-field-maximum ($E_{\max}$) exposure. (b) E and H field distributions of the H-field-maximum ($H_{\max}$) exposure.

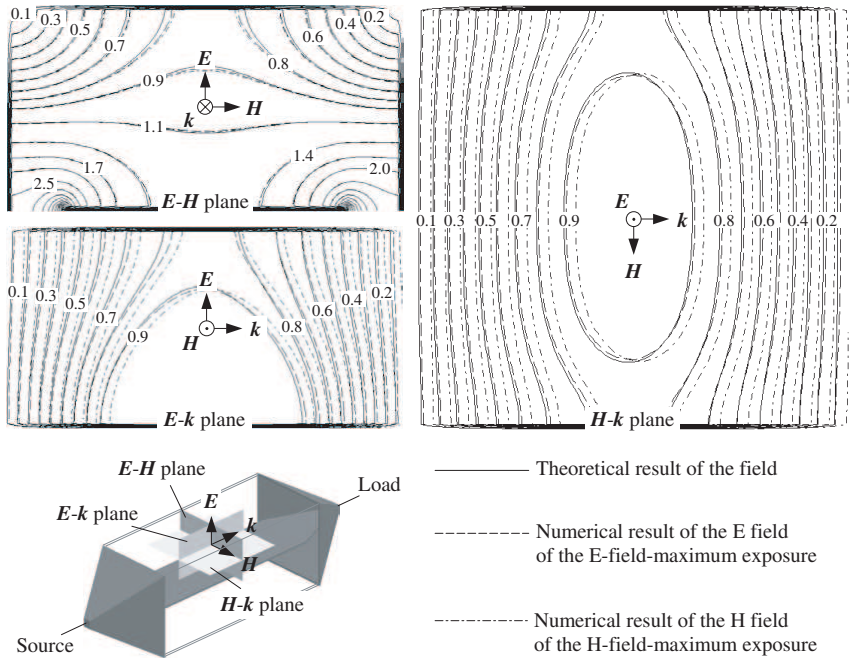

Figure 5. Contour plots of the normalized field distributions in the exposure area, where the direction of the propagation constant ***k*** refers to that of the incident wave from the source. The planes cross the center of the cell culture if the Petri dish was placed.

The results also indicate that, in the area of the Petri dish, the maximum field varies less than 30% from the value at the center. Although the variance is large as compared to the uniform plane wave exposure in the free space, it is to be proved that the nonuniform field has no dominant influence on the SAR heterogeneity. The field uniformity is better for smaller cell containers. However, the SAR heterogeneity increases quickly as the container size is reduced, due to the wave diffraction caused by the geometry variance in limited dimensions, such as the meniscus of the liquid surface. The 35 mm Petri dish is also a compromise selection to reduce the SAR heterogeneity in view of the field uniformity and the container geometry.

4.2. SAR Solution

The voxel size of 0.2 mm is far less than the wavelength of 19.8 mm and skin depth of 7.50 mm in the cell culture. Therefore, the SAR

accuracy is mainly influenced by the inherent numerical dispersion of the FDTD calculation, which is a complicated combined error from the voxel dimensions, time increment, the volume of the problem space, material geometry and dielectric parameters, etc. We examine the SAR solution by using a sphere of cell culture with a diameter of 33.0 mm exposed to the 1800 MHz plane wave. The sphere is dimensionally comparable to the cell culture in the Petri dish. The numerical SAR is calculated in the sphere by the FDTD program. The theoretical SAR in the sphere is obtained by using the Mie theory of the plane-wave scattering problem [22]. In both cases, the power density of the plane wave is 1.0 mW/cm^2. The comparison in Fig. 6 shows a good agreement between the numerical and theoretical results of the SAR distributions through the sphere.

4.3. Temperature Solution

The same cell-culture sphere is used to test the accuracy of the temperature solution. The exposure-induced heating and the heat convection from the sphere to the surrounding air finally result in a stabilized distribution of the maximum temperature rise. With a homogeneous SAR distribution of 0.1 W/kg, the temperature rise along the diameter of the sphere is calculated numerically and analytically [23]. The results are compared in Fig. 7 with a good match. Since the accuracy of the numerical temperature solution is sensitive to the staircase effect at the sphere-air interface, we additionally reduce

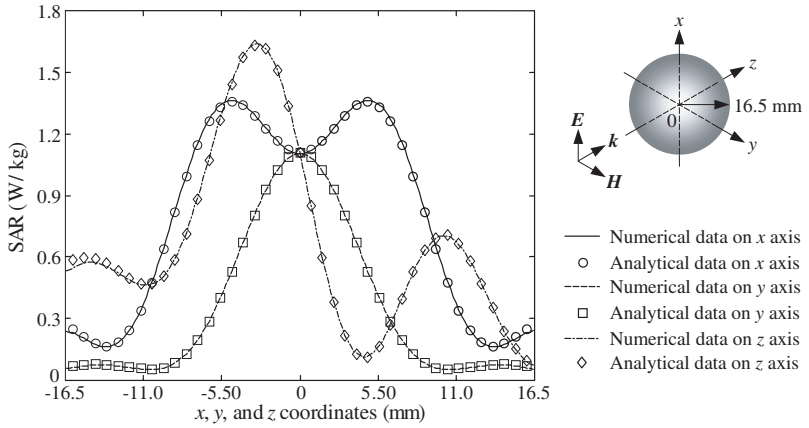

Figure 6. SAR distributions along three orthogonal axes through the 33.0 mm cell-culture sphere exposed to 1.0 mW/cm^2 plane wave.

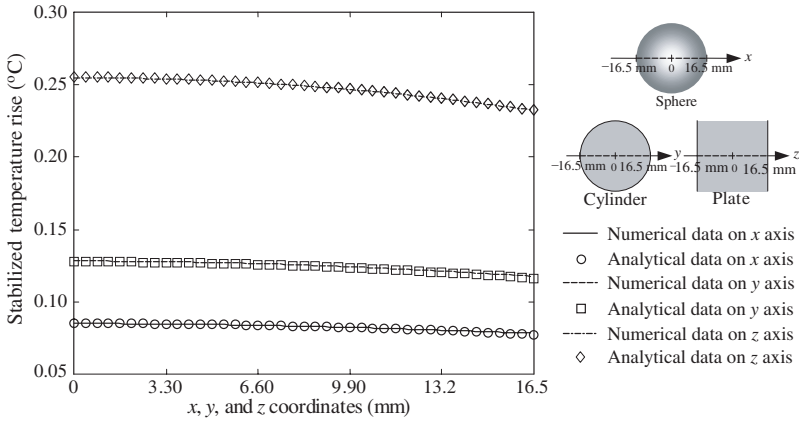

Figure 7. Distributions of the temperature rise through the sphere, cylinder, and plate with 0.1 W/kg homogeneous SAR distribution.

the 3-D problem into 2-D and 1-D problems to strengthen the test. The 2-D model is a cylinder with the same material, diameter, and SAR distribution as those of the sphere. In the 1-D model, the diameter turns into the thickness of a plate. In the additional problems, the numerical and analytical results still match well with each other, as shown in Fig. 7.

5. RESULTS

The FDTD calculation continues for 360 periods of the 1800 MHz sinusoidal wave before the SAR data are collected upon a stable field distribution of the standing wave in the TEM cell. The field stabilization is a transient process of less than 0.2 µs. Therefore, the bioheat calculation directly uses the stabled SAR data to simulate the exposure-induced heating process. The exposure continues for 5 minutes and ends before the temperature distribution becomes steady and the maximum temperature rise is reached in the cell culture.

5.1. Dosimetry Evaluation

The SAR statistics, exposure efficiency and heterogeneity of the 10 exposure arrangements are summarized in Table 2, where the input power of the TEM cell is normalized to 100 mW. The result clearly shows up the dosimetry differences among the arrangements. It is apparent that the exposure with the maximum H field and H orientation of the Petri dish achieves the highest exposure efficiency

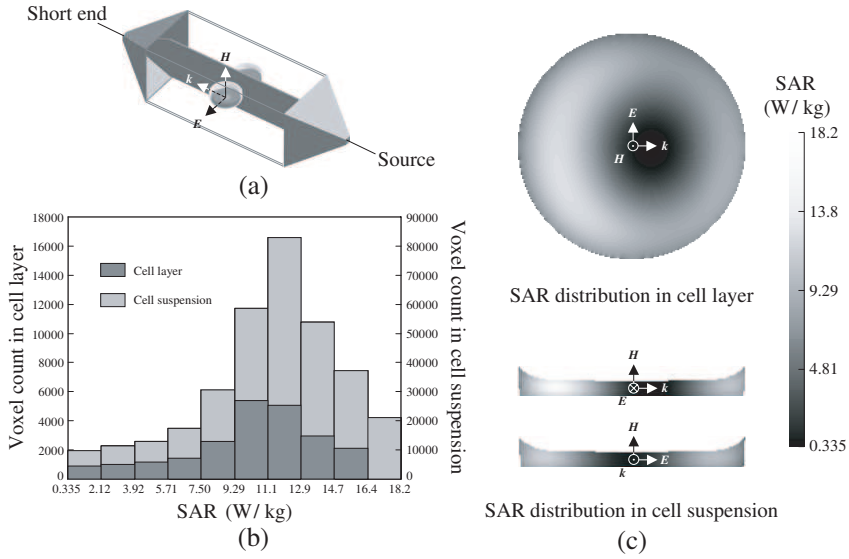

Figure 8. SAR characterization of the selected arrangement with 100 mW input power. (a) Exposure with the maximum H field and H orientation of the Petri dish. (b) Histograms of the voxel count versus the SAR level. (c) SAR distributions in the cell layer and two cuts through the cell suspension.

and the lowest heterogeneity for the cell layer and cell suspension. The exposure efficiency is still good in three other arrangements, namely, the E-field-maximum exposure with the Petri dish orientated in $\boldsymbol{H}$, $\boldsymbol{k}$, and $-\boldsymbol{k}$ directions. However, the exposure heterogeneities are too high and not acceptable. For experiments on the cell layer, the exposure heterogeneity is the lowest in the arrangement of the E-field-maximum exposure and $\boldsymbol{E}$ orientated Petri dish, but the exposure efficiency is too small. The cell suspension inherently absorbs more power and gains higher exposure efficiency than the cell layer. Whereas, the exposure heterogeneity of the cell suspension is generally larger than that of the cell layer because of the complex geometry of the entire liquid.

In an overall view of the exposure efficiency and heterogeneity, the best arrangement is the exposure with the maximum H field and H orientation of the Petri dish. In Fig. 8, the dosimetry is characterized for the selected arrangement with histograms of the voxel count versus the SAR level and images of the SAR distributions in the cell layer and cell suspension. For experiments with this arrangement, the dosimetry evaluation may refer to the shown results with SAR values proportionally adjusted to match input powers other than 100 mW.

Table 2. Comparison of the SAR statistics, exposure efficiency and heterogeneity among various standing wave exposure arrangements with 100 mW input power in the TEM cell.

Exposure on the cell layer with the maximum E field					
Petri dish orientation	$\boldsymbol{E}$	$-\boldsymbol{E}$	$\boldsymbol{H}$	$\boldsymbol{k}$	$-\boldsymbol{k}$
Mean SAR (W/kg)	0.0406	0.0243	9.19	7.18	8.05
SAR SD (W/kg)	0.0143	0.0224	4.77	4.24	4.66
Efficiency (%)	0.00733	0.00438	1.66	1.30	1.45
Heterogeneity (%)	35.2	92.4	51.9	59.1	57.9
Exposure on the cell layer with the maximum H field					
Petri dish orientation	$\boldsymbol{E}$	$-\boldsymbol{E}$	$\boldsymbol{H}$	$\boldsymbol{k}$	$-\boldsymbol{k}$
Mean SAR (W/kg)	0.233	0.147	10.1	0.873	0.153
SAR SD (W/kg)	0.167	0.105	3.59	0.416	0.107
Efficiency (%)	0.0421	0.0266	1.83	0.158	0.0276
Heterogeneity (%)	71.4	71.1	35.4	47.6	70.4
Exposure on the cell suspension with the maximum E field					
Petri dish orientation	$\boldsymbol{E}$	$-\boldsymbol{E}$	$\boldsymbol{H}$	$\boldsymbol{k}$	$-\boldsymbol{k}$
Mean SAR (W/kg)	0.0532	0.0411	9.42	7.76	7.77
SAR SD (W/kg)	0.0737	0.0640	5.18	4.83	4.85
Efficiency (%)	0.141	0.110	25.3	20.8	20.9
Heterogeneity(%)	139	156	54.9	62.2	62.4
Exposure on the cell suspension with the maximum H field					
Petri dish orientation	$\boldsymbol{E}$	$-\boldsymbol{E}$	$\boldsymbol{H}$	$\boldsymbol{k}$	$-\boldsymbol{k}$
Mean SAR (W/kg)	0.161	0.0722	11.2	0.477	0.480
SAR SD (W/kg)	0.147	0.0735	3.77	0.358	0.343
Efficiency (%)	0.426	0.194	30.0	1.28	1.29
Heterogeneity (%)	91.6	102	33.8	75.1	71.3

5.2. Temperature Evaluation

Figure 9(a) records the time-varying temperature rises in the cell layer and the cell suspension. Due to the nonuniform temperature distribution, the records give the maximum values found in the cell culture. The input power of the TEM cell is 40 mW and the selected arrangement is the exposure with the maximum H field and H orientation of the Petri dish. Fig. 9(b) shows distributions of the temperature rise over the cell layer and through the cell suspension at

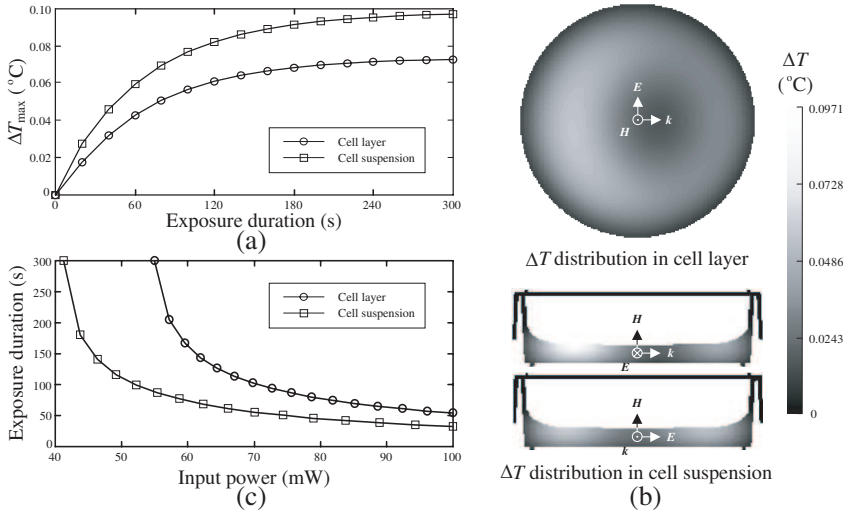

Figure 9. Characterization of the temperature rise of the selected exposure arrangement. (a) Real-time recording of the maximum temperature rises ($\Delta T_{\max}$) in the cell layer and the cell suspension with 40 mW input power. (b) 5-minute exposure-induced temperature rise (ΔT) in cells with 40 mW input power. (c) Limits to the exposure duration with various input powers to prevent cells from being overheated.

the end of the 5-minute exposure. The patterns of the temperature rise are very close to those of the SAR distribution, indicating a limited heat transfer by ways of conduction and convection. The dominant factor in the temperature accumulation is the heat generation due to the energy absorption. The temperature rise is in direct proportion to the input power with the dielectric and thermal parameters of materials remaining constant. Therefore, in a limited range of the temperature variance, e.g., 0.1°C, temperature results from other input powers can be derived from the shown data proportionally.

The temperature rise is a significant concern due to the high exposure efficiency of the selected arrangement. For most bioelectromagnetic experiments interested in nonthermal effects, there is a critical 0.1°C standard of the temperature variance in cells to restrict possible thermal reactions within an undetectable level. Therefore, the exposure duration is to be limited in the experimental protocol to avoid the overheat. Fig. 9(c), for example, gives the maximum exposure duration with respect to the input power for the temperature control with the selected exposure arrangement. If the exposure continues for more than 5 minutes, the temperature

environment will be stable at 520 s, regardless of the various input powers. At the end of the 520 s exposure, the ratios of the maximum temperature rises to the input power in the cell layer and cell suspension are 1.82°C/W and 2.43°C/W, respectively. Therefore, input powers lower than 54.9 mW and 41.2 mW can be used for the cell layer and cell suspension, respectively, with no restriction to the exposure duration while the maximum temperature rise does not exceeds 0.1°C.

5.3. Improvement of the Exposure Quality

Although the exposure with the maximum H field and H orientation of the Petri dish has the best exposure quality among the 10 arrangements, the exposure heterogeneity is still slight higher than the required 30%, being 35.4% and 33.8% in the cell layer and the cell suspension, respectively. Nonstandardized cell containers of smaller dimensions may reduce the exposure heterogeneity but are not recommended for replication studies in different laboratories. Another practical method to improve the exposure quality is to use cells sampled in selected sections in the Petri dish. To facilitate the administration, a ring-shaped plastic film is added to the Petri dish before the cell planting. The cell culture is divided into two sections. In view of the nearly rotational symmetry of the SAR distribution across the middle layer of the cell culture as shown in Fig. 10(a), it is observed that the outer section of the cell culture has higher SAR and lower SAR SD levels. Therefore, the cell sample is taken from this section for better exposure quality. In practice, the cells are seeded in the outer section and the inner section only contains the culture medium.

Because of the power absorption by the cell culture, the reflected wave from the short end is smaller than the wave from the source. Therefore, the SAR distribution in the cell culture is not totally symmetrical along the axis of the TEM cell. The SAR distribution can be improved by using a second source instead of the short end. The second source has the same amplitude as the first source but is 180° out of phase. By this way, the field along the TEM cell axis is totally symmetrical. The SAR distribution in the cell culture from the double-source exposure is shown in Fig. 10(b). The improvement of the SAR symmetry helps to reduce the exposure heterogeneity. However, the double-source exposure uses twice the incident power as that of the single source, so that the exposure efficiency is cut nearly by half.

The exposure quality is tightly related to the size of the outer section containing the cell sample. In Fig. 10(c), the exposure heterogeneity in the cell layer and that in the cell suspension are calculated with respect to the inner radius of the cell samples. The

mean SAR is also provided for each case. A comparison is made between the double-source and single-source exposures. Either for the cell layer or the cell suspension, the double-source exposure is always better than the single-source exposure with lower exposure heterogeneity and higher mean SAR, regardless of the radius. The exposure heterogeneity is mainly caused by the small SAR near the center of the cell samples. With the double-source exposure, the cell layer with the inner radius larger than 2.8 mm fulfills the 30% heterogeneity requirement. The critical radius of the cell suspension is 2.2 mm. For the cell layer with the inner radius of 9.8 mm, the exposure heterogeneity is the lowest as 11.2% and the mean SAR is nearly the highest. For the cell suspension, the best exposure quality with the exposure heterogeneity of 14.4% is found at the radius of 9.6 mm.

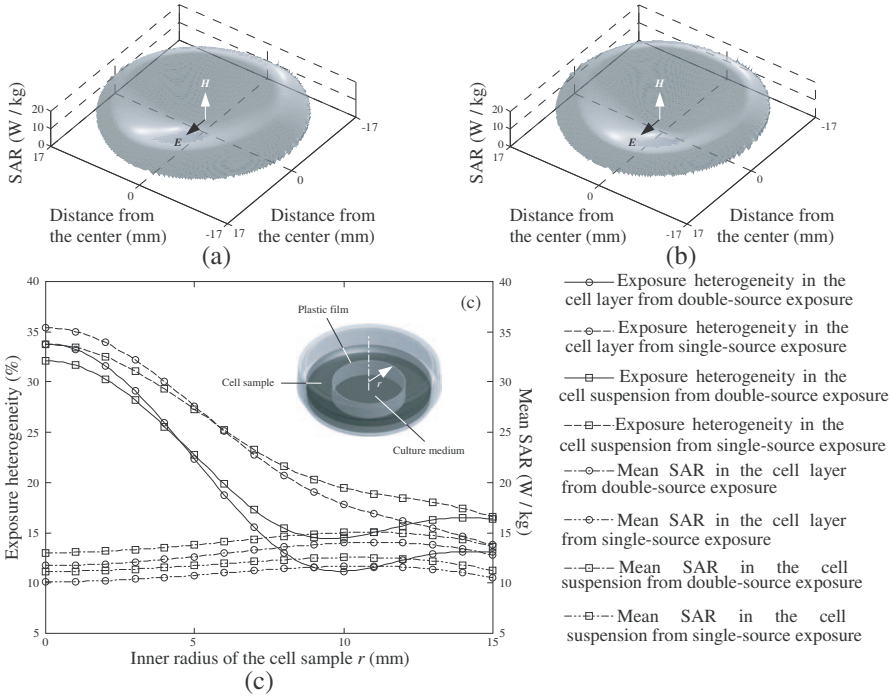

Figure 10. Improvement of the exposure quality. (a) SAR distribution in the middle layer of the cell culture with 100 mW input power from the single-source exposure. (b) SAR distribution in the middle layer of the cell culture with 200 mW input power from the double-source exposure. (c) Exposure heterogeneities and mean SARs versus the inner radius of the cell layer and cell suspension with the single- and double-source exposures.

5.4. Influence of the Holder

Above analysis has neglected the holder of the Petri dish to simplify the problem and address major factors affecting the results. Practically, the Petri dish is positioned in the exposure area by a holder. The holder should have minimum influence on the field distribution, the airflow, and the heat conduction, so that above results of the dosimetry and temperature rise are still valid. This is an important consideration because the holders are nonstandardized components in the exposure setup and various designs may be applied. Low loss material and thin structures are suggested for the holder to minimize the disturbance on the field distribution. The main plate of the holder should be parallel to the axis of the TEM cell to smooth the airflow. At the same time, the holder should grip the Petri dish using the smallest contacting area to reduce the heat conduction as much as possible.

As an example, we have designed a holder according to the above three recommendations. Shown in Fig. 11(a), the holder consists of a shelf adhered by a couple of brackets to the outer conductor of the TEM cell. The material is the same plastic as that of the Petri dish and the thickness is 2.0 mm. The hole in the shelf helps to grip the Petri dish by the ring on its base panel. The contour plots in Fig. 11(b) give the SAR results from the model with the holder and that without the holder when the input power is 200 mW from the double sources. The stabilized temperature rises in both models under 80 mW exposure are shown in Fig. 11(c). The maximum SARs and the maximum temperature rises in the cell layer and cell suspension are listed in Table 3. The comparisons indicate limited variances in the dosimetric and thermal environments caused by the holder.

Table 3. Comparison of the maximum SARs and temperature rises in cells between models with and without the holder.

Cell sample	Cell layer		Cell suspension	
Exposure setup	With holder	Without holder	With holder	Without holder
Maximum SAR (W/kg)[a]	17.3	16.4	19.8	19.0
Maximum temperature rise (°C)[b]	0.0709	0.0705	0.0921	0.0941

[a]Exposure with the incident power of 200 mW from the double source.

[b]Exposure with the incident power of 80 mW from the double source.

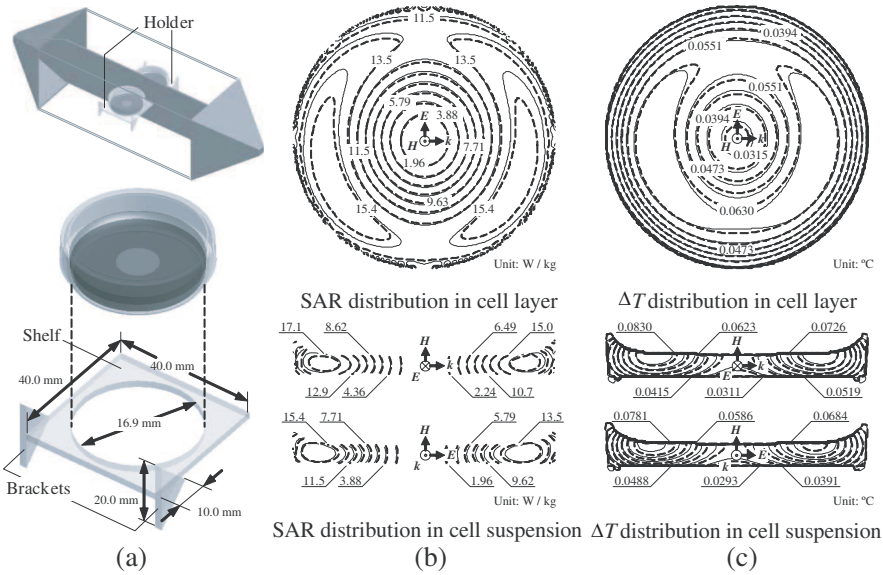

Figure 11. Influences of the holder on the SAR and temperature rise. (a) Geometry of the holder. (b) SAR distributions in the cell layer and two cuts through the cell suspension with 200 mW input power from the double sources. (c) Stabilized temperature rises in cells induced by 80 mW exposure. In (b) and (c), the solid and dashed lines are results from the models with and without the holder, respectively.

6. DISCUSSION

The proposed exposure setup is featured by the combination of the TEM cell and the standing wave exposure. Besides the above dosimetry and temperature rise evaluations to quantify and characterize the setup, the following comparisons demonstrate the exposure quality improvement of the novel design over traditional ones.

6.1. Comparison between the TEM Cell and the Waveguide

At frequencies above 1 GHz, most exposure setups use the waveguide as the microwave applicator. Relatively little dosimetric work about the TEM cell in the frequency range around 1800 MHz is available in the literature [24]. In Table 4, we made a comparison between the 1800 MHz TEM cell and the waveguide on the dosimetry and temperature results. Both the TEM cell and the waveguide use the standing wave exposure on the 35 mm Petri dish. Dosimetry and temperature data from the waveguide are obtained from the literature

Table 4. Comparison of the dosimetry and temperature environments between the TEM cell and the waveguide.

Cell sample	Cell layer		Cell suspension	
Exposure setup	TEM cell	Waveguide	TEM cell	Waveguide
Normalized mean SAR [(W/kg)/W][a]	101	196[c]	112	230[c]
Heterogeneity (%)	35	33[c]	34	117[e]
Normalized maximum temperature rise [°C/(W/kg)][b]	0.018	0.022[d]	0.022	0.11[e]

[a]Data are normalized to the incident power of 1 W.

[b]Dara are normalized to the mean SAR in the cell sample.

[c]Value from 1950 MHz H-field-maximum exposure on a single $\boldsymbol{H}$-orientated Petri dish.

[d]Value from 1800 MHz H-field-maximum exposure on multiple $\boldsymbol{E}$-orientated Petri dishes.

[e]Value from 1800 MHz E-field-maximum exposure on multiple $\boldsymbol{E}$-orientated Petri dishes.

at the frequencies of 1950 MHz and 1800 MHz loaded with single or multiple Petri dishes [25, 26]. The dosimetry data are adjusted to comply with the 2.68 ml cell culture used in this study, according to the relation between the SAR and the culture volume [27].

The normalized mean SAR is a unified measure to compare the exposure efficiency among different exposure setups. The TEM cell has the normalized mean SAR about half that of the waveguide. However, it is noticed that the TEM cell exposes double Petri dishes simultaneously, while the waveguide in the comparison contains one dish. Therefore, the exposure efficiency is overall the same between the TEM cell and the waveguide. For experiments on the cell layer, the exposure efficiency of the TEM cell is a slight higher than that of the waveguide, but the exposure heterogeneity is also higher. On the contrary, in the case of cell suspension, the TEM cell has a lower exposure efficiency and lower heterogeneity than those of the waveguide. The temperature control with the TEM cell is easier since the temperature rise is less sensitive to the SAR accumulation than

that of the waveguide, as indicated by the maximum temperature rise normalized to the mean SAR. In the comparison, the maximum temperature rise is obtained upon the stabilization of the thermal environment.

The dosimetry and temperature differences between the cell layer and cell suspension are obviously smaller in the TEM cell than those in the waveguide. Therefore, the TEM cell has a better performance with less positional variance of the exposure condition. This is a beneficial quality for experiments in which the cell position is uncertain in the culture medium.

6.2. Comparison between the Standing Wave Exposure and the Propagating Wave Exposure

Applications of the TEM cell to in vitro experiments have used the propagating wave exposure. In the exposure area where the Petri dish is absent, the power flux density (PFD) of the propagating wave varies over the cross section but keeps constant along the axis of the TEM cell. Whereas the PFD of the standing wave changes from its peak value to zero along the axis over 1/8 of a wavelength. Therefore, an exposure with a lower heterogeneity is achieved by using the propagating wave in the empty TEM cell. However, with the presence of the Petri dish, the exposure quality is not only determined by the incident field, but mainly refers to the total field in the cell culture. In Table 5, we list the dosimetry data for the propagating wave exposure. The data are obtained by using previous models revised by using a $50\,\Omega$ matching load instead of the open end or short end. In any case of the Petri dish orientations and the cell formations, the efficiency of the propagating wave exposure is much lower than the standing wave exposure as the above selected one, whereas the exposure heterogeneity of the propagating wave is significantly higher.

The power absorption is described as the inductive coupling between the H field and the cell culture, as well as the capacitive coupling between the E field and the cell culture [28]. In this study, the selected arrangement has the maximum H field and the minimum E field in the exposure area. Therefore, the inductive coupling is dominant in the cell culture. With the nearly uniform H field, the coupled E field increases from the center to the border of the cell culture. The H orientation of the Petri dish provides the largest area for the increase and reduces the overall gradient of the E field, which benefits the reduction of the exposure heterogeneity.

The TEM cell with the standing wave exposure has a very limited exposure area. Cell containers of larger sizes, such as the T25 flask, is not applicable. Enlarging the cross section of the TEM cell could

Table 5. SAR statistics, exposure efficiency and heterogeneity among various propagating wave exposure arrangements with 100 mW input power in the TEM cell.

Exposure on the cell layer					
Petri dish orientation	$\boldsymbol{E}$	$-\boldsymbol{E}$	$\boldsymbol{H}$	$\boldsymbol{k}$	$-\boldsymbol{k}$
Mean SAR (W/kg)	0.0703	0.0431	6.07	2.83	3.00
SAR SD (W/kg)	0.0414	0.0308	3.29	1.57	1.81
Efficiency (%)	0.00634	0.00389	1.10	0.256	0.270
Heterogeneity (%)	58.9	71.5	54.3	55.5	60.6
Exposure on the cell suspension					
Petri dish orientation	$\boldsymbol{E}$	$-\boldsymbol{E}$	$\boldsymbol{H}$	$\boldsymbol{k}$	$-\boldsymbol{k}$
Mean SAR (W/kg)	0.0546	0.0282	6.41	2.91	3.00
SAR SD (W/kg)	0.0517	0.0276	3.55	1.85	1.81
Efficiency (%)	0.072	0.0380	17.2	3.91	4.03
Heterogeneity (%)	94.7	98.0	55.3	63.6	60.3

lead to the generation of other modes and is not suggested. However, the TEM cell can be extended along the axis and so is the standing wave. For experiments with a large volume of the cell sample, 4, 6, and more 35 mm Petri dishes can be used and placed periodically along the extended TEM cell at H maximum positions to receive the exposure. The study of multiple exposed objects is in succession.

7. CONCLUSION

We have introduced a 1800 MHz exposure setup for bioelectromagnetic studies. The setup is characterized by the standing wave exposure in the TEM cell. Based on the numerical quantification and characterization of the dosimetry and temperature rise in cells cultured in the Petri dish, the study searches for the best exposure quality with the highest exposure efficiency and the lowest exposure heterogeneity. We compare the results from the TEM cell and the waveguide, those from the standing wave exposure and the propagating wave exposure, as well as the results among various standing wave exposures combined from the maximum fields and the orientations of the Petri dish. The systematic comparison concludes that the TEM cell with the maximum H field exposure of the standing wave and the H orientation of the

Petri dish is the optimal exposure setup for in vitro experiments at 1800 MHz.

ACKNOWLEDGMENT

The study is funded by the National Natural Science Foundation of China under grant No. 30700148, the Fundamental Research Funds for the Central Universities under grant No. JY10000902005, and is also supported under grant No. 2007F08 by the Natural Science Foundation of Shaanxi Province.

REFERENCES

1. Schönborn, F., K. Poković, M. Burkhardt, and N. Kuster, "Basis for optimization of in vitro exposure apparatus for health hazard evaluations of mobile communications," *Bioelectromagnetics*, Vol. 22, 547–559, Dec. 2001.
2. Paffi, A., F. Apollonio, M. Liberti, R. Pinto, and G. A. Lovisolo, "Review of radiofrequency exposure systems for in vitro biological experiments," *Proceedings of the Fourth European Conference on Antennas and Propagation (EuCAP)*, 1–4, Barcelona, Spain, Apr. 2010.
3. Nikoloski, N., J. Fröhlich, T. Samaras, J. Schuderer, and N. Kuster, "Reevaluation and improved design of the TEM cell in vitro exposure unit for replication studies," *Bioelectromagnetics*, Vol. 26, 215–224, Apr. 2005.
4. Popović, M., S. C. Hagness, and A. Taflove, "Finite-difference time-domain analysis of a complete transverse electromagnetic cell loaded with liquid biological media in culture dishes," *IEEE Trans. on Biomed. Eng.*, Vol. 45, 1067–1076, Aug. 1998.
5. IEEE Standard for Safety Levels with Respect to Human Exposure to Radio Frequency Electromagnetic Fields, 3 kHz to 300 GHz, IEEE C95.1-2005, 2005.
6. Kusuma, A. H., A.-F. Sheta, I. Elshafiey, Z. Siddiqui, M. A. S. Alkanhal, S. Aldosari, S. A. Alshebeili, and S. F. Mahmoud, "A new low SAR antenna structure for wireless handset applications," *Progress In Electromagnetics Research*, Vol. 112, 23–40, 2011.
7. Zhao, J. X., "Numerical dosimetry for cells under millimetre-wave irradiation using Petri dish exposure set-ups," *Phys. Med. Biol.*, Vol. 50, 3405–3421, Jul. 2005.

8. Kuster, N. and F. Schönborn, "Recommended minimal requirements and development guidelines for exposure setups of bioexperiments addressing the health risk concern of wireless communications," *Bioelectromagnetics*, Vol. 21, 508–514, Oct. 2000.
9. Paffi, A., F. Apollonio, G. A. Lovisolo, C. Marino, R. Pinto, M. Repacholi, and M. Liberti, "Considerations for developing an RF exposure system: A review for in vitro biological experiments," *IEEE Trans. on Microwave Theory and Tech.*, Vol. 58, 2702–2714, Oct. 2010.
10. Samaras, T., P. Regli, and N. Kuster, "Electromagnetic and heat transfer computations for non-ionizing radiation dosimetry," *Phys. Med. Biol.*, Vol. 45, 2233–2246, Aug. 2000.
11. Schönborn, F., K. Poković, A. M. Wobus, and N. Kuster, "Design, optimization, realization, and analysis of an in vitro system for the exposure of embryonic stem cells at 1.71 GHz," *Bioelectromagnetics*, Vol. 21, 372–384, Jul. 2000.
12. Andrews, E. F., H. B. Lim, D. Xiao, S. Khamas, P. L. Starke, S. P. Ang, A. T. Barker, G. G. Cook, L. A. Coulton, and A. Scutt, "Investigation of SAR uniformity in TEM cell exposed culture media," *IEE Antenna Measurements and SAR, AMS*, 71–74, Loughborough, United Kingdom, May 2004.
13. Boriraksantikul, N., P. Kirawanich, and N. E. Islam, "Near-field radiation from commercial cellular phones using a TEM cell," *Progress In Electromagnetics Research B*, Vol. 11, 15–28, 2009.
14. Prisco, G. D., G. d'Ambrosio, M. L. Calabrese, R. Massa, and J. Juutilainen, "SAR and efficiency evaluation of a 900 MHz waveguide chamber for cell exposure," *Bioelectromagnetics*, Vol. 29, 429–438, Sep. 2008.
15. Crawford, M. L., "Generation of standard EM fields using TEM transmission cells," *IEEE Trans. on Electromagn. Compat.*, Vol. 16, 189–195, Nov. 1974.
16. Zhao, J. X. and Z. G. Wei, "Numerical dosimetry for cells cultured in Petri dishes exposed to a six-degree-freedom millimeter-wave radiator," *Journal of Electromagnetic Waves and Applications*, Vol. 19, No. 9, 1183–1197, 2005.
17. Taflove, A., *Computational Electrodynamics: The Finite-difference Time-domain Method*, Artech House, Boston, MA, 1995.
18. Pennes, H. H., "Analysis of tissue and arterial blood temperatures in the resting human forearm," *J. Appl. Physiol.*, Vol. 1, 93–122, Aug. 1948.

19. Schuderer, J., D. Spät, T. Samaras, W. Oesch, and N. Kuster, "In vitro exposure systems for RF exposures at 900 MHz," *IEEE Trans. on Microwave Theory and Tech.*, Vol. 52, 2067–2075, Aug. 2004.
20. Bernardi, P., M. Cavagnaro, S. Pisa, and E. Piuzzi, "SAR distribution and temperature increase in an anatomical model of the human eye exposed to the field radiated by the user antenna in a wireless LAN," *IEEE Trans. on Microwave Theory and Tech.*, Vol. 46, 2074–2082, Dec. 1998.
21. Kong, J. A., *Electromagnetic Wave Theory*, Wiley, New York, 1990.
22. Zhao, J. X., "Numerical and analytical formulizations of the extended Mie theory for solving the sphere scattering problem," *Journal of Electromagnetic Waves and Applications*, Vol. 20, No. 7, 967–983, 2006.
23. Shih, T. M., *Numerical Heat Transfer*, Hemisphere, New York, 1984.
24. Guy, A. W., C. K. Chou, and J. A. McDougall, "A quarter century of in vitro research: A new look at exposure methods," *Bioelectromagnetics*, Vol. 20, 21–39, 1999.
25. Calabrese, M. L., G. d'Ambrosio, R. Massa, and G. Petraglia, "A high-efficiency waveguide applicator for in vitro exposure of mammalian cells at 1.95 GHz," *IEEE Trans. on Microwave Theory and Tech.*, Vol. 54, 2256–2264, May 2006.
26. Schuderer, J., T. Samaras, W. Oesch, D. Spät, and N. Kuster, "High peak SAR exposure unit with tight exposure and environmental control for in vitro experiments at 1800 MHz," *IEEE Trans. on Microwave Theory and Tech.*, Vol. 52, 2057–2066, Aug. 2004.
27. Schuderer, J. and N. Kuster, "Effect of the meniscus at the solid/liquid interface on the SAR distribution in Petri dishes and flasks," *Bioelectromagnetics*, Vol. 24, 103–108, Feb. 2003.
28. Burkhardt, M., K. Poković, M. Gnos, T. Schmid, and N. Kuster, "Numerical and experimental dosimetry of Petri dish exposure setups," *Bioelectromagnetics*, Vol. 17, 483–493, 1996.